C. ALLAN BOYLES and GERALDINE W. JOICE

COMPARISON OF THREE ACOUSTIC TRANSMISSION LOSS MODELS WITH EXPERIMENTAL DATA

The use of sound is a basic part of antisubmarine warfare. One factor affecting submarine detection is transmission loss, which is a measure of the extent to which sound is weakened in passing from one point to another. In the deep ocean, an important propagation mode is convergence zone propagation. When it exists, the sound intensity does not decay as fast with range because the sound energy is partially focused. This article compares the latest theoretical models with measured transmission loss data taken under the conditions of convergence zone formation.

INTRODUCTION

Since acoustic or sound waves propagate more readily than electromagnetic waves through water, the use of sound has become a basic part of antisubmarine warfare technology since World War II. There are always many different ways in which equipment can be designed and used, and an intelligent choice among the alternatives depends on accurate knowledge of the different factors affecting performance. One of these factors is the extent to which sound is weakened in passing from one point to another. This weakening is called transmission loss. It is possible to arrive at a suitable choice of equipment and operational doctrine experimentally by trial-and-error methods, but this can be extremely costly and time consuming. Different equipment must be designed, built, taken to sea, and tested under a wide range of weather and oceanographic conditions. It is much quicker and less expensive if theoretical models can be used to guide the decision as to which is the optimum type of equipment and operational doctrine to be employed for any circumstance. The theoretical predictions, of course, cannot be divorced from the experimental data. A limited number of sea tests must be conducted in order to confirm the validity of the theoretical models.

This article describes one phase of a sea test conducted in April 1976 in the Pacific Ocean. The major objective of that phase was to make detailed, accurate transmission loss measurements and supporting oceanographic measurements so that values derived using the latest theoretical models could be compared with the measured values.

Two ships participated in the test: the R/V *Seismic Explorer* (Fig. 1), which towed the receiving hydrophone, and the USNS *DeSteiguer* (Fig. 2), which towed the acoustic projector and took extensive oceanographic measurements. The receiving hydrophone used to measure the transmission loss was a simple omnidirectional hydrophone. (Omnidirectional means that the response of the hydrophone to an arriving sound wave is independent of the arrival direction.) The acoustic projector (Fig. 3) is quite large, weighing approximately 2600 pounds in air. A series of eight tonals or sine waves and a linear fre-

Figure 1 — The R/V *Seismic Explorer* was used to tow the receiving hydrophone.

Figure 2 — The USNS *DeSteiguer* was used to tow the acoustic projector and perform various oceanographic measurements.

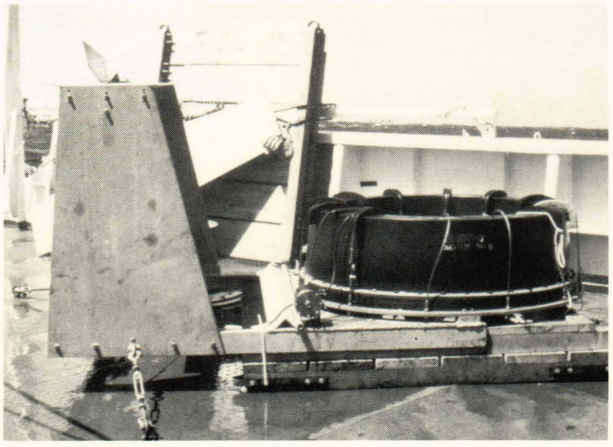

Figure 3 — The acoustic projector used to generate the comb of eight sine waves and the linear frequency-modulated signal. The projector is quite large and weighs about 2600 pounds.

quency-modulated signal were radiated by the projector. In this article, only the 550-hertz tonal and the linear frequency-modulated signal are discussed.

The oceanographic parameters measured during the test were temperature and salinity as functions of depth, and the speed of sound measured directly. Very few direct measurements of the sound speed were made because the ship had to remain stationary for several hours while a velocimeter was lowered by cable to the bottom. Figure 4 shows the velocimeter being lowered. Temperature measurements can be made from a moving ship by using a temperature probe called an expendable bathythermograph. The probe is launched from a tube and trails a very fine wire over which the signal carrying the temperature information is continually transmitted. Figure 5 shows a temperature probe being launched during the test. Because the speed of sound depends on temperature, salinity, and pressure (or, equivalently, depth), it can be computed from measurements of temperature and salinity. Since seawater is nondispersive at frequencies of interest in antisubmarine warfare (through the megahertz range), the speed of sound discussed above is the phase velocity.

Prior to World War II, only crude listening devices and echo ranging devices were in use. That war gave the real impetus to research in underwater acoustics. Since then, some remarkable advances have been made in the field of underwater sound. One such area has been a detailed investigation of the temperature structure of the deep ocean and the many different propagation paths available to sound energy over very long ranges (hundreds of kilometers). One important mode of propagation is called convergence zone propagation. Where convergence zones exist, sound energy does not decay as rapidly with range as it otherwise would because the energy is partially refocused. The physics of convergence zone formation will be discussed in the next section.

In order to measure transmission loss in a convergence zone environment, two ships that are initially

Figure 4 — The Navy oceanographer aboard the USNS *DeSteiguer* prepares to lower a sound velocimeter. This instrumentation package measures the speed of sound directly as a function of depth and also measures temperature and salinity.

separated by only a few nautical miles open the range between them until they are about 185 kilometers apart. There are three convergence zones within a range of 185 kilometers. Figure 6 is an artist's conception of a typical run. In this article, we will only examine the data taken in the first convergence zone.

CONVERGENCE ZONE FORMATION

In order to gain some understanding of deep ocean acoustic propagation and convergence zone formation, consider the simplified sound speed profile shown in Fig. 7. Here we have plotted the speed of sound versus water depth from the sea surface to the bottom of the water column.

Suppose there is a point source at a depth of 100 meters. (A point source has dimensions much smaller than the wavelength being radiated and emits spherical wave fronts.) Figure 8 shows two infinitesimal ray bundles leaving the source in a downward direction. Rays are curves that are always perpendicular to wave fronts and, in the limit of vanishing wavelength, energy is transported in the direction of the rays. It is incorrect to speak about intensity or power per unit area along a single ray. Therefore, associated with each ray is an infinitesimal area of the wave

Figure 5 — An expendable bathythermograph probe immediately after launch. Notice the very fine wire, trailing from the probe, over which data are transmitted to a recorder. In contrast to the sound velocimeter shown in Fig. 4, these probes can be launched from a moving ship.

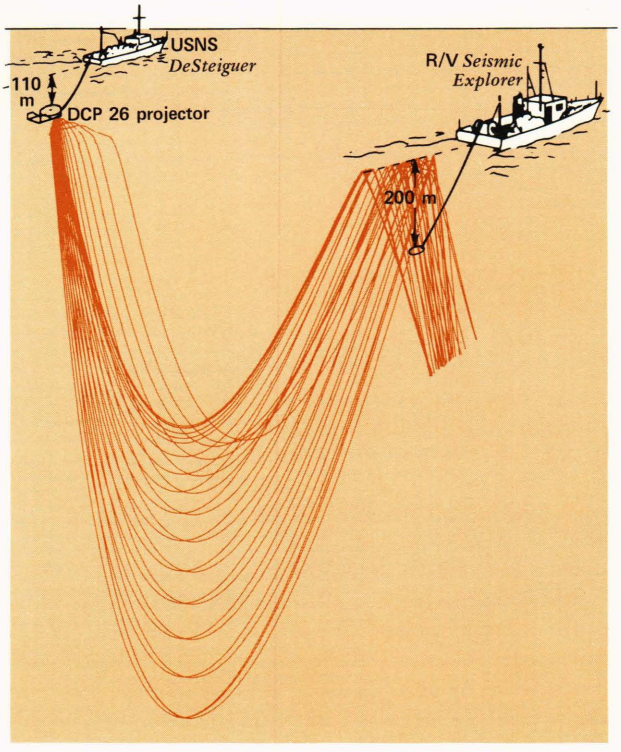

Figure 6 — An artist's conception of an opening run to measure transmission loss.

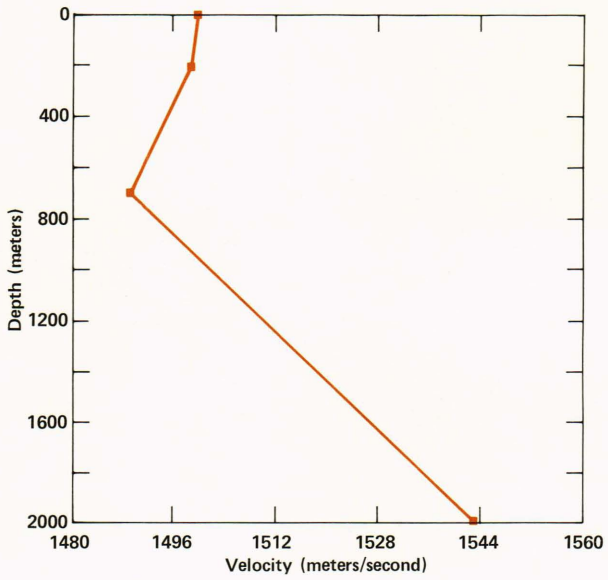

Figure 7 — Sound velocity as a function of depth. This simplified profile is used to illustrate the formation of convergence zones.

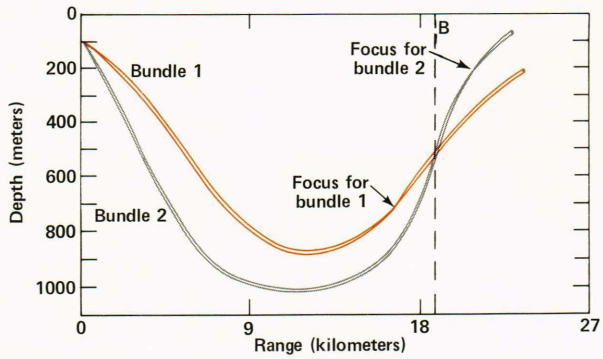

Figure 8 — Example of how two (of many) ray bundles focus to create local regions of high intensity.

front about that ray and perpendicular to it. The collection of all rays that go through this small area of wave front is called the infinitesimal ray bundle associated with the original ray. The trajectory of the ray bundle describes how a small but finite area of the wave front is refracted. In the ray theory approximation, the energy is confined to a ray bundle. Leakage of energy out of the bundle is called diffraction.

Ray bundles leaving a point source initially start out along a radial line from the source because the wave fronts are spherical close to the source and the rays are perpendicular to the wave fronts. Before long, they are bent or refracted by the inhomogeneous medium. Why this refraction takes place is easy to see. Consider, for example, a bundle leaving the source horizontally at a depth of 100 meters. Reference to Fig. 7 shows that the speed of sound is decreasing with depth in that region. The top of the small wave front subtended by the bundle is moving at a faster speed than the bottom of the wave front. Hence, the rays through the wave front would tend to

be refracted downward. The same reasoning can be used to explain upward refraction if the speed of sound is increasing with depth.

The diameters of the bundles shown in Fig. 8 have been greatly exaggerated for clarity. Bundle 1 focuses relatively soon after its lower vertex. (Focusing means that the small portion of the wave front subtended by the ray bundle collapses to a point and then expands as it moves away from the focal point.) Bundle 2, leaving the source at a steeper grazing angle (the angle between the ray and the horizontal), focuses later at a shallower depth. Ray bundles leaving the source at angles between those of bundles 1 and 2 will have focal points located between the focal points of bundles 1 and 2. The locus of all the focal points is termed the caustic surface. In the ray theory approximation (i.e., for vanishing wavelength), the intensity at the caustic is infinite. The important thing to note is that, whereas not all the wave front is focused, small areas of the wave front are individually focused at different points, giving rise to high-intensity regions called convergence zones.

Figure 9 shows a ray trace for many rays leaving the source in a downward direction. Each bundle is represented by a single ray. The envelope of the rays after a single refraction is the caustic surface. Note that to the left of the caustic there is a shadow zone (i.e., a region of zero intensity in the ray theory approximation) only for the totality of ray bundles that forms the caustic. In general, there will be other ray bundles that get into the shadow zone, but none will have a focal point on the caustic.

Next, consider the multipath structure behind the caustic in what we call the illuminated region (Fig. 10). Consider a receiver being towed at a depth of 400 meters. The ray bundle that leaves the source at an angle of 5.5° down from the horizontal focuses at 400 meters and forms the caustic there. To the left of that point is the shadow zone. To the right of the caustic, two ray bundles go through each point. (A ray bundle is represented by a single ray in Fig. 10 and in all ray diagrams that follow.) One such range point (viz., point B) is illustrated in Fig. 10. One bundle leaves the source at a grazing angle (here 3.9°) less than that of the caustic-forming bundle, and the other leaves the source at a grazing angle (here 7.4°) greater than that of the caustic-forming bundle. Point B here corresponds to point B of Fig. 8. It is seen that, for the receiver at point B, one ray bundle has already focused before arriving at B. Therefore, in addition to a phase difference resulting from the relative travel times, there will be an additional 90° phase shift of bundle 1 relative to bundle 2 because a wave front undergoes a $-90°$ phase shift when it goes through a focal point. In the region around a focal point, the ray theory approximation breaks down. Physically, this means that diffracted energy is not negligible and the flow of energy is no longer confined to the ray tube but leaks out of it. The interference between the energy flowing along the ray tube and the diffracted energy creates the $-90°$ phase shift.

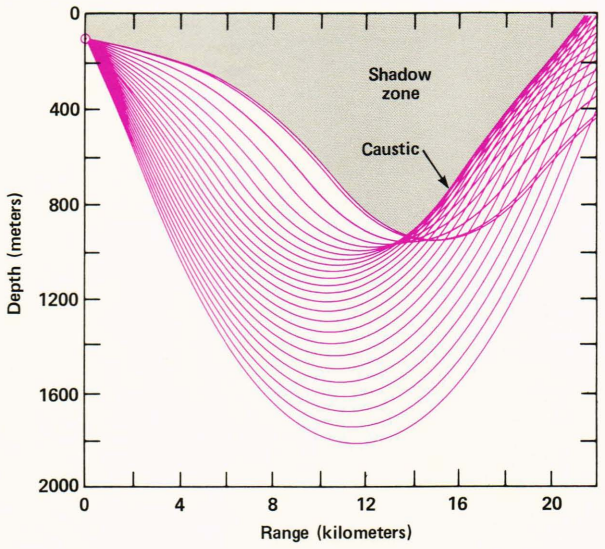

Figure 9 — A ray plot of a smooth caustic. The caustic is the envelope of the rays shown.

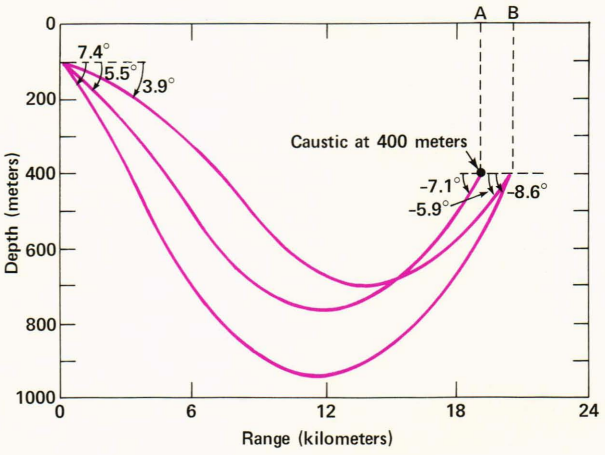

Figure 10 — Two-ray system behind a smooth caustic. Two rays pass through each point for some distance behind and at the same depth as the caustic.

The transmission loss is the loss in intensity of sound between a point 1 yard from the source and a receiver at some arbitrary distance from the source. If I_0 is the wave intensity at 3 feet and I is the intensity at the receiver, the transmission loss between the reference distance of 3 feet from the source and the distant receiver is:

$$\text{transmission loss} = 10 \log (I_0/I), \text{ decibels.} \quad (1)$$

Figure 11 shows transmission loss as a function of range for a range interval about the caustic. This plot is for a frequency of 550 hertz. The vertical dashed line is the location of the caustic. The transmission loss shown by the solid curve is calculated from ray theory, which predicts zero intensity in the shadow zone and infinite intensity on the caustic. The lobing structure behind the caustic is caused by the interference of the two rays interacting in and out of the

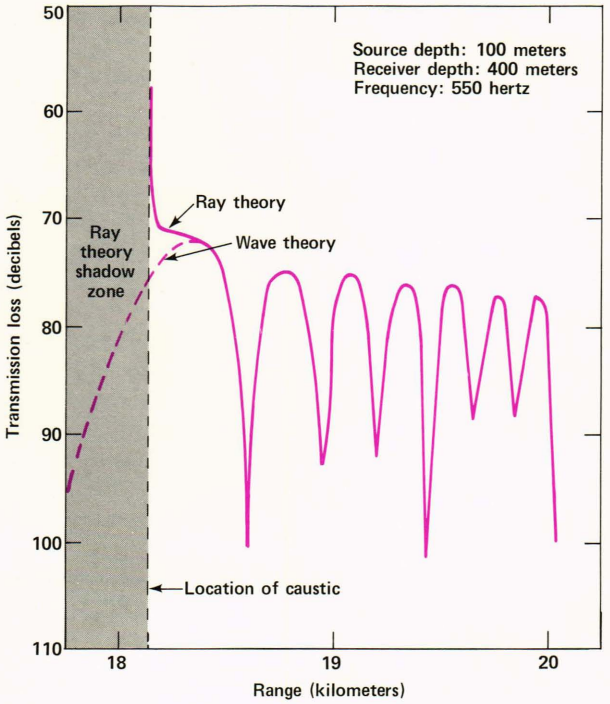

Figure 11 — Transmission loss measured in decibels as a function of range from the source. The source depth is 100 meters, the receiver depth is 400 meters, and the frequency is 550 hertz. The caustic is located at a range of 33.5 kilometers. The solid curve is the transmission loss determined by ray theory. It shows infinite intensity at the caustic and no energy to its left (the shadow zone). The dashed curve is the correct transmission loss determined by wave theory. According to wave theory, the maximum intensity is behind the caustic.

phase. The infinite intensity at the caustic results from the vanishing wavelength approximation of ray theory. The more rigorous wave theory must be used to calculate the correct, finite intensity. The transmission loss resulting from wave theory is shown by the dashed curve. Note that the maximum intensity is behind the caustic and not on it. This condition is the result of the 90° phase shift of one ray relative to the other. Also note that wave theory predicts energy diffracted into the shadow zone.

DESCRIPTION OF THEORETICAL PROPAGATION MODELS

In this section, we describe briefly the three propagation models that were compared with measurements. The models are standard and are used widely throughout the acoustic community.

Continuous Gradient Ray Tracing System (CONGRATS)

CONGRATS, the work of Weinberg,[1] is a range-independent, fully coherent ray-trace model used to compute transmission loss as a function of range and frequency at fixed source and receiver depths.

The model used for the ocean environment is horizontally layered; i.e., the sound velocity is a function of water depth only and does not vary with range. In addition, the bottom is assumed to be flat and the water depth constant. The sound velocity profile is approximated by a continuous piecewise linear fit so that within each layer the sound velocity gradient is constant. Within the water column, the frequency-dependent volume attenuation as calculated by Thorp[2] is included.

The ocean bottom is modeled as a reflecting surface where each ray suffers a reflection loss that depends on grazing angle, frequency, and bottom type. Bottom type is input to the CONGRATS program so that any data may be used. No phase shift is associated with reflection from the ocean bottom. The ocean surface, however, is modeled as a perfect reflector with a $-180°$ phase shift for all rays.

CONGRATS first traces those rays specified in the input data by their source angle and number of reversals. If a particular type of ray does not go through the receiver position, the program interpolates between two rays of the same history that bracket the receiver position. Those that go from source to receiver are called eigenrays. For each eigenray, the program calculates its source angle, arrival angle, travel time, transmission loss, total phase, phase shifts, and number of reversals. The total phase along a ray is $\omega T + \phi$, where $\omega/2\pi$ is the frequency, T is the travel time, and ϕ is the cumulative phase shift of $-\pi$ radians when the ray reflects off the sea surface and $-\pi/2$ radians if the ray touches a caustic. After all eigenrays at one receiver location have been found, the program adds them coherently (i.e., as complex numbers, taking amplitude and phase into account) and gives the total transmission loss.

Blatstein[3,4] made extensive additions to the original CONGRATS program by incorporating into it Sach's and Silbiger's[5] asymptotic wave solution for the treatment of smooth caustics.

The Fast Asymptotic Coherence Transmission (FACT) Model

FACT[6] is a ray acoustics model developed by Spofford to compute transmission loss as a function of range and frequency at fixed source and receiver depths. The classic ray treatment has been augmented with high-order asymptotic corrections and the phased addition of selected paths.

The model used for the ocean environment is "layered," i.e., is a function of depth only. Neither the sound velocity profile nor the bottom depth is range dependent. The sound velocity profile is approximated by a continuous piecewise linear function of depth so that the sound speed gradient is constant within each layer but is discontinuous at layer boundaries. Within the water column, a frequency-dependent volume attenuation is included. This treatment corresponds to Thorp's absorption above 1 kilohertz and is an empirical result derived by Fleet Numerical Weather Central below 1 kilohertz.

The ocean bottom is modeled as a reflecting surface where each ray suffers reflection loss that de-

pends on grazing angle, frequency, and bottom class. The loss suffered as a function of these parameters is given by Fleet Numerical Weather Central bottom loss tables for frequencies less than 1 kilohertz or greater than 3.5 kilohertz and by the new Naval Oceanographic Office Navy Standard Curves from 1 to 3.5 kilohertz. The ocean surface is modeled as a perfect reflector (with a $-180°$ phase shift) for all rays considered.

To compute the total transmission loss, FACT does not do a phased sum of the ray amplitudes. The phase along a ray is never computed in FACT. With two exceptions (surface-image interference effects and caustics), all ray paths are summed incoherently. The justifications offered for this approximation are that the phased sum oscillates quite rapidly with range and that the uncertainties in the geometry and the environment preclude an accurate estimate of phase. For most applications, the oscillations are too rapid to be useful in detail and should be smoothed. What is needed, then, is a range-averaging technique that smooths the rapid fluctuations while preserving long-term significant departures from the root-mean-square sum of all paths. These long-term departures result primarily from long-range surface-image interference effects, for which an approximate calculation is used to phase sum the appropriate paths.

FACT treats smooth caustics as well as cusp caustics. It uses the root-mean-square average of the Pearcey function[7] to treat cusp caustics.

Parabolic Equation (PE) Model

The PE method was introduced into underwater acoustics by Tappert and Hardin[8] in 1972. They developed an efficient integration algorithm to evaluate the parabolic approximation[9,10] to the full elliptic wave equation.

The basic idea of the PE method is to replace the elliptic wave equation by a parabolic partial differential equation, which has a unique, stable solution for Dirichlet and Neuman type boundary conditions on an open surface. This characteristic makes the equation amenable to a marching solution when the initial conditions are known.

The solution of the parabolic wave equation includes diffraction and all other full-wave effects such as the rigorous treatment of caustics. However, the approximation made to obtain the parabolic wave equation does put some restriction on the solution. McDaniel[11] examined the effect of the parabolic approximation on the propagation of normal modes in a layered but range-independent ocean. She showed that discrete modes are propagated with the correct amplitudes and mode shapes but with errors in the phase and group velocities. These errors can cause substantial shifts in the modal interference pattern. The PE program used at APL, supplied by Science Application, Inc., employs a technique developed by Brock, Buchal, and Spofford[12] to reduce the effect of the phase-velocity error.

Further, the PE solution properly accounts for full-mode coupling only to the extent that backscattering is negligible, which it frequently is in acoustic propagation in the ocean.

In order to start up the PE program, the acoustic field at some range over the entire depth mesh must be supplied. This input can be generated by a normal mode program. However, the APL version of the program is initiated with a digital low-pass filter for a source function that was developed by Garon, Hanna, and Rost.[13]

One last feature peculiar to the APL model should be mentioned. The ocean bottom is made highly absorbing, so that no bottom interaction energy returns to the water column. This feature was implemented to attenuate the bottom-interacting modes that may be in considerable error owing to the particular integration algorithm used in the numerical implementation of the model.

The attenuation coefficients used in PE for the water column are the same as those used in FACT.

COMPARISON OF THEORETICAL AND EXPERIMENTAL TRANSMISSION LOSSES AND MULTIPATH STRUCTURE IN THE FIRST CONVERGENCE ZONE

Transmission losses calculated by CONGRATS, FACT, and PE were compared with experimental transmission losses at the single frequency of 550 hertz for the first convergence zone. In addition, the multipath structure measured in the first convergence zone was compared with that calculated by CONGRATS.

The experimental transmission loss data were recorded on analog tapes that were processed on the Sonar Processing System at APL, where a 4096-point fast Fourier transform was performed to provide narrowband analysis. The processing was performed on 0.5-hertz bins and required 2-second transforms. The resultant processed data were then dumped onto digital 9-track tapes for plotting. Consequently, the curve of measured transmission loss versus range represents a record of a contiguous sequence of 2-second samples. No incoherent averaging was performed on the transmission loss data.

The sound velocity profile used for the transmission loss modeling is shown in Fig. 12. Using this profile, which was actually measured at sea during the test, we generated a CONGRATS ray diagram for the rays propagating from a 110-meter source out to the first convergence zone (Fig. 13). This zone is formed after the rays have experienced a deep refraction that takes place at approximately 28 kilometers in the ray plot. For a receiver depth of 200 meters, the zone extends from about 46 to 68 kilometers.

Figure 14 shows the five distinct ray families that primarily compose the first convergence zone. Families 1 and 2 are formed by refracted-refracted rays that are totally trapped in the water column and have

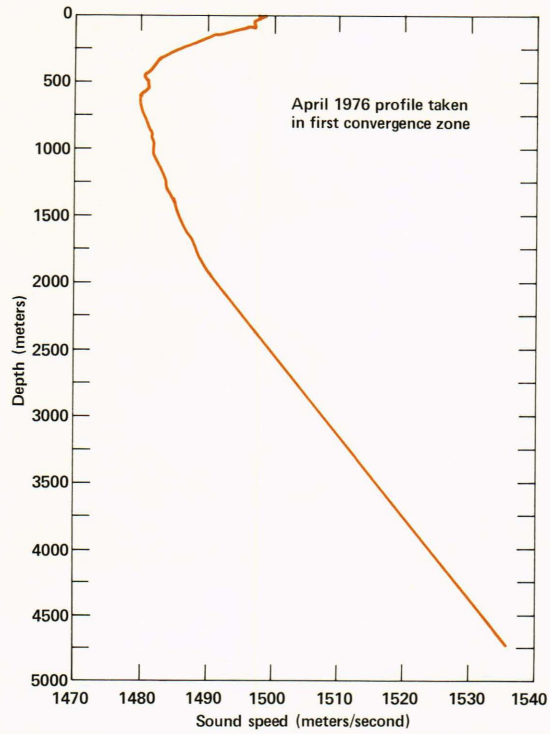

Figure 12 — Sound speed profile measured during the sea test and used for transmission loss calculations by the modified CONGRATS, PE, and FACT models.

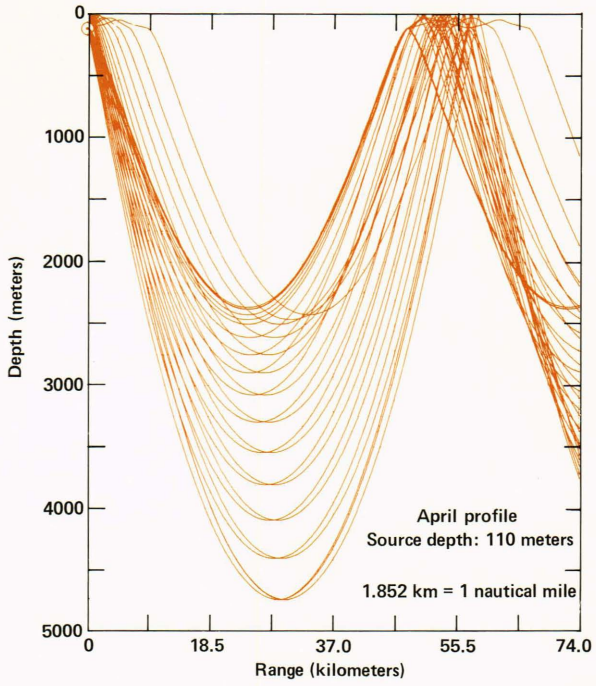

Figure 13 — Ray trace generated by CONGRATS using the sound speed profile of Fig. 12. Note the formation of the convergence zone from approximately 37 to 74 kilometers and the presence of the shadow zone in front of the convergence zone.

not interacted with either boundary prior to encountering the receiver. Families 3, 4, and 5 are formed by refracted surface-reflected rays that have encountered the surface at least once but have not interacted with the bottom. While bottom-interacting rays also enter the first convergence zone, their contribution is negligible because of the attenuation imposed on the rays by the acoustic properties of the bottom. Further, because of the benign sea conditions during the test, the sea surface was fairly calm. Thus, any scattering caused by a rough surface (scattering that is not treated by the models) is also negligible.

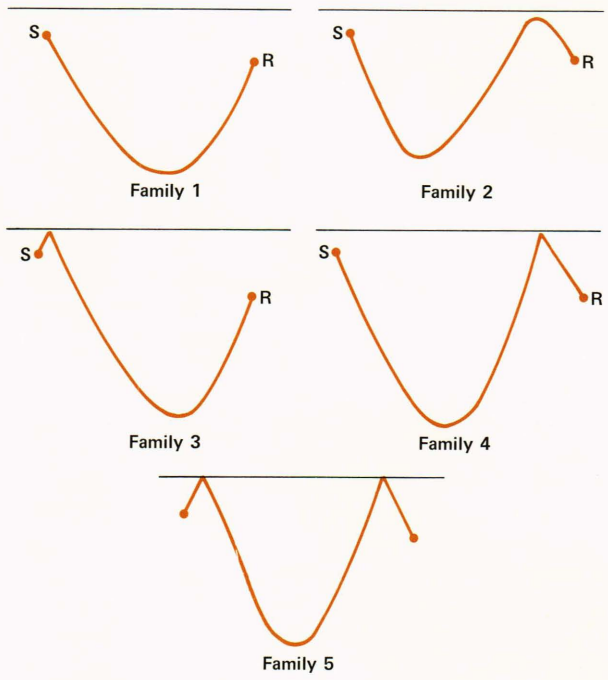

Figure 14 — Five primary ray families composing the first convergence zone. Note that families 1 and 2 have traversed totally within the water column and have not encountered the surface or the bottom prior to arriving at the receiver, whereas families 3, 4, and 5 have encountered the surface at least once prior to arriving at the receiver.

Figure 15 compares the first convergence zone multipath structure measured by linear frequency modulation techniques with that predicted by CONGRATS for a source depth of 110 meters and a receiver depth of 200 meters. To obtain the measured multipath structure, the relative travel times of a 500- to 2000-hertz linear frequency-modulated ramp signal (2-second period) propagated over various paths in the first convergence zone were determined to better than 1-millisecond resolution. (The relative travel time is the absolute travel time along the ray, minus the horizontal range between the source and the receiver, divided by the reference sound speed.) The measured multipath structure is shown in the lower portion of Fig. 15. The upper part of the figure is a plot of relative travel time versus range for the rays arriving at a single hydrophone as calculated by CONGRATS. The five distinct families are indeed observed in the multipath structure. It is also observed that CONGRATS does an excellent job of predicting the multipath structure.

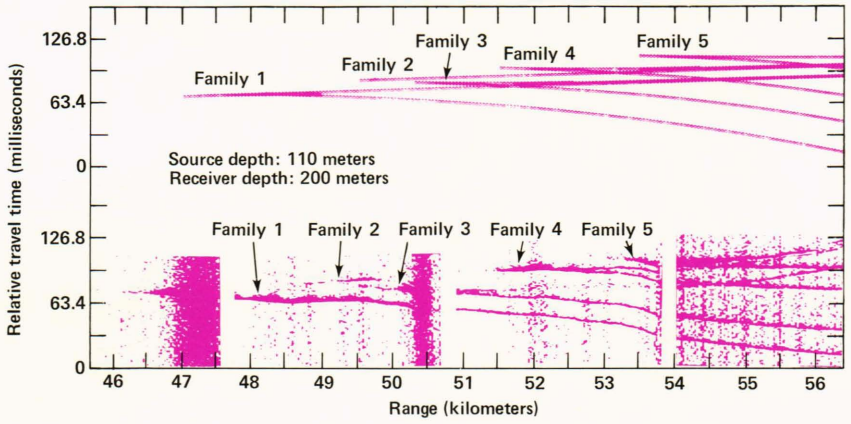

Figure 15 — Comparison of the measured and theoretical (CONGRATS) multipath structure in the first convergence zone. The agreement is excellent, and all five families of Fig. 14 are observed.

In addition to showing the relative travel time between arrivals, the measured multipath data show the intensity level of the ray paths and the energy diffracted into the ray theory shadow zone. Neither the intensity level nor the diffracted energy is shown on the upper plot generated by CONGRATS. Consequently, some of the ray paths seen in the measured data disappear earlier than the CONGRATS ray paths because of low intensity. Family 2 is an example. Ray theory calculations confirm that all of these arrivals are weak and should not be seen in the measured multipath data. CONGRATS predicts that the intensity in Family 2 should peak strongly in a narrow range interval and should then fall off rapidly; this behavior is what is actually seen in the measured data. The other phenomenon observed in the measured multipath data, but not in the CONGRATS plot, was the diffracted energy in the shadow zone at a caustic. To illustrate, we see that Family 1 starts at a range of 46.95 kilometers on the CONGRATS plot. This is the range at which the first real rays of the convergence zone begin. The measured multipath plot shows considerable energy extending to the left of this range, corresponding to the diffracted field in the shadow zone of the first caustic. While this diffracted energy is not shown in the relative time plot generated by CONGRATS, it is calculated by CONGRATS and does appear in the CONGRATS transmission loss plots.

Figures 16, 17, and 18 compare the measured first convergence zone transmission loss versus range relationship with those calculated by modified CONGRATS, PE, and FACT, respectively. The range scale corresponds to the measured transmission loss. The large discrepancy between the measured transmission loss and that calculated by PE in the bottom-bounce region in front of the first convergence zone results from assuming a totally absorbing bottom in PE.

To compare the predicted and measured transmission loss levels for the first convergence zone, a statistical approach was adopted. Consider M data values of the transmission loss, x_i, $i = 1,\ldots, M$. The probability density function, $p(x)$, of x can be estimated by

$$\hat{p}(x) = M_x/MW\,, \tag{2}$$

where W is a narrow interval centered at x and M_x is the number of data values that fall within the range $x = \pm W/2$. Note that the estimate $\hat{p}(x)$ is not unique since it clearly depends on the number of intervals and their width. Certainly as the interval width, W, decreases and as the number of data values, M, increases, the estimate approaches the probability density function:

$$p(x) = \lim_{\substack{M\to\infty \\ w\to 0}} \hat{p}(x)\,. \tag{3}$$

The cumulative probability distribution function can be obtained from the probability density estimate.

Probability density and probability distribution histograms were constructed using the measured and predicted transmission loss values from the first 7.85 nautical miles of the first convergence zone. The transmission loss data were accumulated in 1-decibel bins. Figure 19 compares the distribution functions for the measured and the PE-generated transmission loss data. The comparison was ascertained in the following manner. For a given percentile level, say 10%, one finds from the distribution curves that 10% of the measured transmission loss samples have a value less than 77.5 decibels and that 10% of the PE transmission loss samples have a value less than 78.5 decibels. This difference between the theoretical and experimental transmission loss values (viz., 78.5 − 77.5 = 1 decibel at the tenth percentile) was obtained from all percentiles. Across all percentile levels, PE is within 1 decibel of the measured transmission loss, and CONGRATS is within 1.5 decibels. FACT was determined to be unsuitable for such a detailed percentile comparison because of the averaging implicit in the FACT transmission loss data.

CONCLUSIONS

A primary objective of the sea test was to establish an experimental transmission loss data base for model comparison and validation. This objective was certainly achieved. The analysis of a portion of the

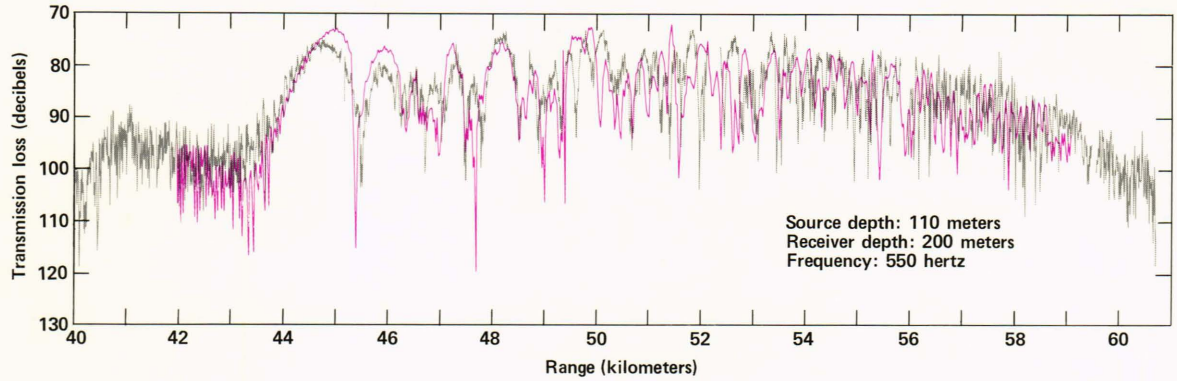

Figure 16 — Comparison of the measured transmission loss data with data calculated by CONGRATS for the first convergence zone. Agreement in the transmission loss levels and in the transmission loss lobing structure is quite good.

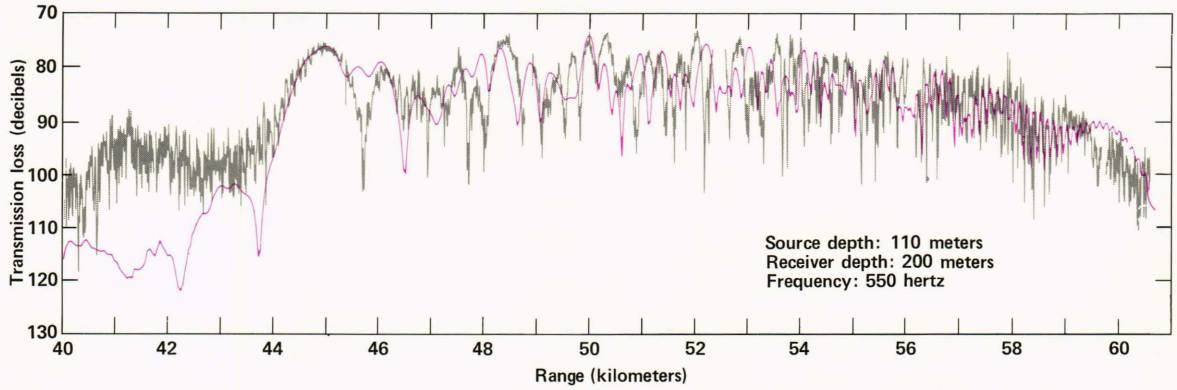

Figure 17 — Comparison of the measured transmission loss data with data calculated by PE for the first convergence zone. Agreement in the transmission loss levels and the transmission loss lobing structure is quite good.

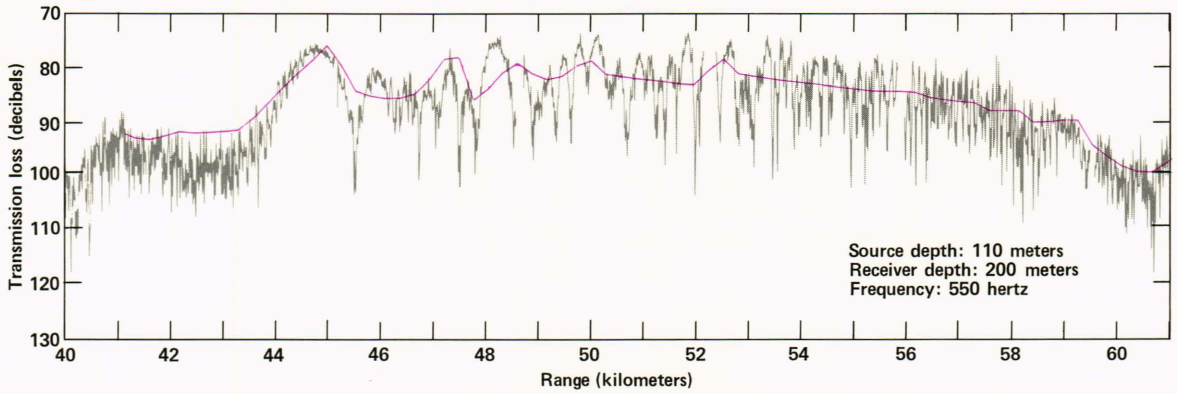

Figure 18 — Comparison of the measured transmission loss data with data calculated by FACT for the first convergence zone. Because of the averaging inherent in FACT, the detailed lobing structure observed in the measured transmission loss is not predicted by the model. The FACT transmission loss levels appear to predict, on the average, the measured transmission loss levels, but discrepancies of more than 10 decibels are observed. In general, FACT does not agree with the data as well as CONGRATS and PE do.

data base, the first convergence zone transmission loss at 550 hertz, has been presented here. The measured transmission loss data were recorded continually at sea and were subsequently processed using 0.5-hertz resolution, yielding 2-second sampling. This detailed transmission loss data base, coupled with the establishment of the concomitant measured multipath structure, permitted a detailed analysis of the different paths present in the first convergence zone and of the transmission loss structure resulting from coherently summing the different paths. While some comparisons of modeled and experimental transmission loss data have been performed prior to this particular work, this is the most extensive comparison to

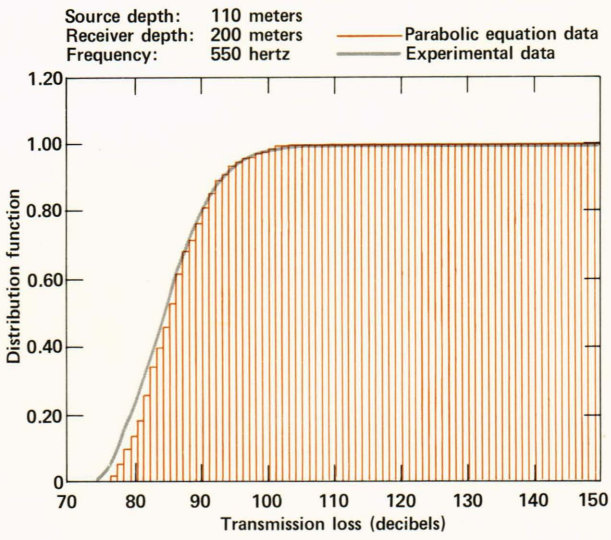

Figure 19 — Comparison of the measured transmission loss distribution function with that predicted by PE for the first convergence zone. Across all percentiles, PE agrees with the measured data to within 1.0 decibel.

date and the first joint comparison of the measured and modeled transmission losses and multipath structures.

The three compared models are currently being used extensively in the community. Therefore, knowledge of their validity in various environments is desired. If one considers the results presented here, both PE and modified CONGRATS did an excellent job of predicting transmission loss and multipath structure in the first convergence zone. Across all percentiles, PE agreed with the measured data to within 1.0 decibel and CONGRATS agreed to within 1.5 decibels. Since the first convergence zone is composed primarily of paths that are completely contained within the water column and do not interact with the bottom, both PE and modified CONGRATS were found to be excellent models for treating this waterborne energy. Note that modified CONGRATS only treats diffraction into the shadow zone at a caustic whereas PE treats full wave diffraction effects. For that reason, and considering cost and convenience, PE is the preferred model.

The agreement between the FACT transmission loss and the measured transmission loss was considerably poorer. Discrepancies of greater than 10 decibels were observed. The poor agreement results from the averaging inherent in the FACT data. For this reason, the detailed percentile comparison was determined to be unsuitable for this case.

Source and receiver depths were possible sources of error in this analysis. However, fairly accurate depth sensors were used during the test. Further, the comparison of modeled and measured multipath structure was invaluable in determining the precise source and receiver depths. Similarly, any range variability in the sound speed along the propagation track is also a source of error. Consequently, multiple profiles measured along the propagation track were input to PE, and the resulting transmission loss was compared with the measured transmission loss. The use of multiple profiles in this case did not significantly improve the comparison.

In conclusion, both PE and modified CONGRATS were excellent models for the prediction of transmission loss in the first convergence zone. They were subjected to a detailed comparison with densely sampled, measured transmission loss data. The less ambitious FACT model exhibited fairly poor agreement with the measured data. Of the three models, PE was preferred because of the excellent agreement with the experimental data, the treatment of full diffraction effects in the model, and the relative ease in using the model.

REFERENCES

1. H. Weinberg, *CONGRATS I: Ray Plotting and Eigenray Generation*, NUSC Report 1052 (Oct 1969).
2. W. H. Thorp, "Deep Ocean Sound Attenuation in the Sub- and Low-Kilocycle-per-Second Region," *J. Acoust. Soc. Am.* **38**, 648-654 (1965).
3. I. M. Blatstein, *Comparison of Normal Mode Theory, Ray Theory, and Modified Ray Theory for Arbitrary Sound Velocity Profiles Resulting in Convergence Zones*, NOLTR 74-95 (29 Aug 1974).
4. I. M. Blatstein and J. A. Goertner, *Prediction Techniques for Refraction of Underwater Explosion Shock Waves*, NOLTR 74-142 (8 Nov 1974).
5. D. A. Sachs and A. Silbiger, "The Focusing and Refraction of Harmonic Sound and Transient Pulses in Stratified Media," *J. Acoust. Soc. Am.* **49**, 824-840 (1971).
6. C. W. Spofford, *The FACT Model*, Maury Center for Ocean Sciences, Report 109 (Nov 1974).
7. L. M. Brekhovskikh, *Waves in a Layered Media*, Academic Press, New York, pp. 483-492 (1960).
8. F. D. Tappert and R. H. Hardin, "Applications of the Split Step Fourier Method to the Numerical Solutions of Nonlinear and Variable Coefficient Wave Equations," *SIAM Rev.* **423(A)** (1973).
9. V. A. Fock, *J. Phys. USSR* **10**, 399-409 (1964).
10. M. A. Leontovich and V. A. Fock, *J. Phys. USSR* **10**, 13-24 (1964).
11. S. T. McDaniel, "Propagation of Normal Mode in the Parabolic Approximation," *J. Acoust. Soc. Am.* **57**, 307-311 (1975).
12. H. K. Brock, R. N. Buchal, and C. W. Spofford, "Modifying the Sound Speed Profile to Improve the Accuracy of the Parabolic Equation Technique," *J. Acoust. Soc. Am.* **62**, 543-552 (1977).
13. H. M. Garon, J. S. Hanna, and P. V. Rost, "Construction of a New Source Function for the Parabolic Equation Algorithm," *J. Acoust. Soc. Am.* **61S**, S12(A) (1977).

ACKNOWLEDGMENT — The authors wish to acknowledge A. M. Diamant and G. D. Tyler, Jr., both of APL, for processing and analyzing the measured transmission loss data, and L. H. Wallman formerly of APL, for processing and analyzing the measured multipath structure.